

RESEARCH LETTERS

Adaptive Optics and Spectral-Domain Optical Coherence Tomography of Human Photoreceptor Structure After Short-Duration Pascal Macular Grid and Panretinal Laser Photocoagulation

To understand the effect of therapeutic doses of laser application on the neurosensory retina, detailed histologic¹⁻³ and optical coherence tomographic (OCT)⁴⁻¹⁰ evaluations have been used in both animal models and the human eye. We sought to evaluate photoreceptor structure associated with laser photocoagulation lesions using 2 high-resolution retinal imaging tools: adaptive optics (AO) and spectral-domain OCT (SD-OCT).

Methods. Two patients received short-duration (20-millisecond) Pascal laser therapy (532 nm; Opti-Medica Corp) for clinical indications. Subject 1 was a 57-year-old woman with macular edema from hemispherical retinal vein occlusion. Treatment consisted of 3×3 grid laser applications with a 100- μ m spot diameter and 100- μ m spacing using 100 mW of power and a 20-millisecond duration to produce barely visible lesions clinically. Subject 2 was a 43-year-old woman with proliferative diabetic retinopathy treated with panretinal laser photocoagulation consisting of 4×4 grid arrays with a 200- μ m spot diameter and 200- μ m spacing using 425 mW of power and a 20-millisecond duration to produce lesions of moderate intensity (eFigure 1, <http://www.archophthalmol.com>). For calibration of all retinal images, axial length was measured using an IOLMaster (Carl Zeiss Meditec). The Pascal system delivered evenly spaced laser applications with clinical precision, facilitating our investigation in these patients. Institutional review board approval was obtained.

SD-OCT Imaging. Volumetric SD-OCT images of the macula were obtained using SD-OCT (Biotigen, Inc) and Cirrus high-definition OCT (Carl Zeiss Meditec). Volumes were nominally 6×6 mm and consisted of 128 B-scans (512 A-scans per B-scan). Cirrus software version 5.0 was used to create C-scans (en face reconstructions)

from the macular volumes to aid in coregistration with other images.

AO Retinal Imaging. Images of the photoreceptor mosaic were obtained using an AO flood-illuminated camera¹¹ and/or an AO scanning ophthalmoscope (AOSO).¹² Rod and cone densities were estimated using a semiautomated direct counting procedure.¹³ Lesion size was estimated manually as the edge-to-edge distance of the disruption of the photoreceptor mosaic (AO) or the disruption of the photoreceptor layers (SD-OCT).

Results. *Subject 1.* The AO imaging was successful after edema regressed. The correlation between B-scan and C-scan SD-OCT images, color fundus photographs, and an AOSO montage of the photoreceptors in the area of macular grid laser treatment was determined (**Figure 1A-D** and **Figure 2**). On AOSO, circular zones of hyporeflectivity with uniform absence of photoreceptors corresponded to laser lesions observed by SD-OCT and color fundus photographs. Photoreceptor disturbances appeared to correspond to the area of laser application and not beyond it.

The mean (SD) size of 20 lesions on AOSO was 92.0 (10.9) μ m, with substantial variability in their appearance (eFigure 2). In an area between 2 lesions, we observed an undisturbed photoreceptor mosaic of 82 819 rods/mm² and 8658 cones/mm². Both of these values are consistent with normal values from the same system.¹² The areas absent of photoreceptors corresponded in size to the areas of photocoagulation, indicating that photoreceptor cell migration into the laser lesion was limited or absent.

Subject 2. The SD-OCT images of representative panretinal laser photocoagulation lesions and surrounding areas are shown in Figure 1E and F. The AO images of the photoreceptor mosaic and lesion are shown in **Figure 3**. Lesions consisted of circular areas of central hyperreflectivity surrounded by a ring of hyporeflectivity (Figure 3B), corresponding to the central hyperpigmented areas and surrounding concentric rings of hypopigmentation, respectively (Figure 3A). Diffusely high reflectivity was observed at the margins of some of the lesions (Figure 3D and F). The cone mosaic appeared normal immediately adjacent to the lesion (Figure 3E and F). The cone density at a nearby location was 8732 cones/mm², consistent with normal values for this eccentricity (Figure 3C). The approximate mean (SD) diameter of the panretinal laser photocoagulation lesions was 306 (43.2) μ m (5 lesions evaluated),

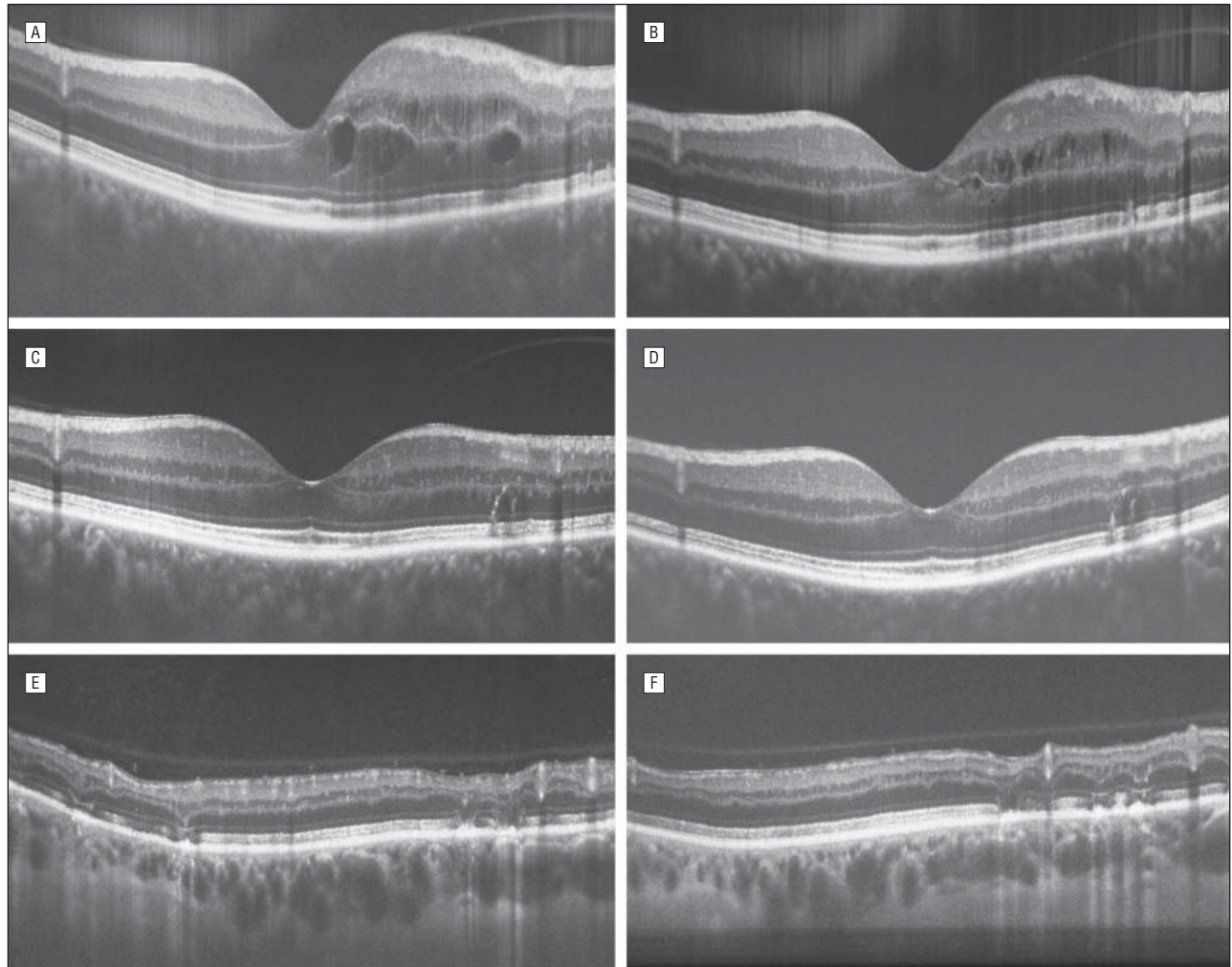


Figure 1. Appearance of laser lesions on spectral-domain optical coherence tomography. Subject 1 was imaged 25 days (A), 74 days (B), 249 days (C), and 341 days (D) after laser treatment. Macular edema 25 and 74 days after treatment was of sufficient severity to inhibit reliable imaging of photoreceptors with the adaptive optics flood-illuminated system. Clear images of the photoreceptor mosaic surrounding the laser lesions were obtained with the adaptive optics scanning ophthalmoscope 341 days after treatment. At the later times, the spectral-domain optical coherence tomographic images demonstrate disturbance of the outer photoreceptor layers and development of a hyperreflective structure in the outer nuclear layer in areas of laser treatment. Subject 2 was imaged 142 days (E) and 236 days (F) after laser treatment. In both images, disturbance of the outer photoreceptor layers is visible.

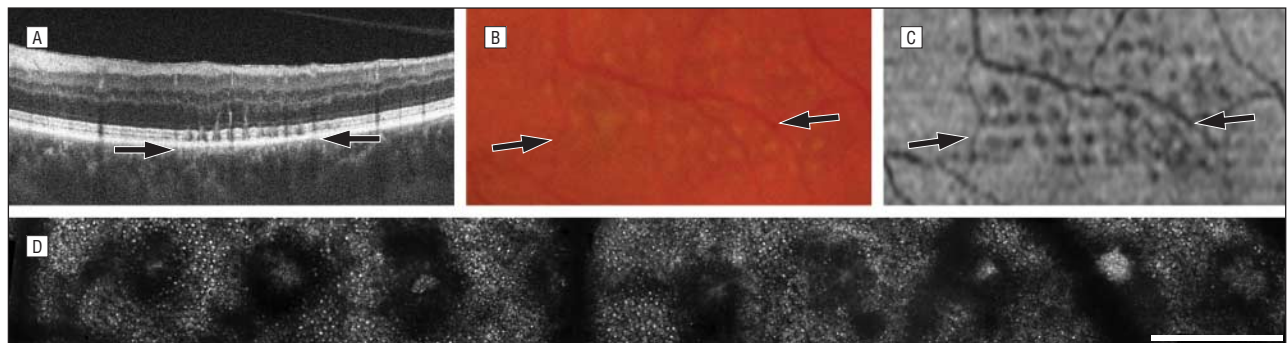


Figure 2. Images from subject 1 showing correlation of B- and C-scan spectral-domain optical coherence tomographic images with fundus appearance and adaptive optics scanning ophthalmoscopy of the photoreceptor layer 341 days after macular grid laser treatment and resolution of macular edema. Images consist of horizontally oriented B-scan acquired using the Biotigen spectral-domain optical coherence tomographic system (A), a cropped area from a color fundus photograph (B), and a corresponding C-scan image acquired with the Cirrus high-definition optical coherence tomographic system (C). D, Adaptive optics scanning ophthalmoscopy montage of these 9 lesions. Scale bar indicates 200 μ m. The boundaries of this montage are indicated by the arrows in A-C.

with precise measurements limited by somewhat ill-defined lesion borders. While cones (and sometimes the smaller rods) can be visualized in Figure 3C, E, and

F, the hyperreflective spots in Figure 3B are likely not photoreceptors, illustrating a challenge in interpreting AO-derived images of the cone mosaic.

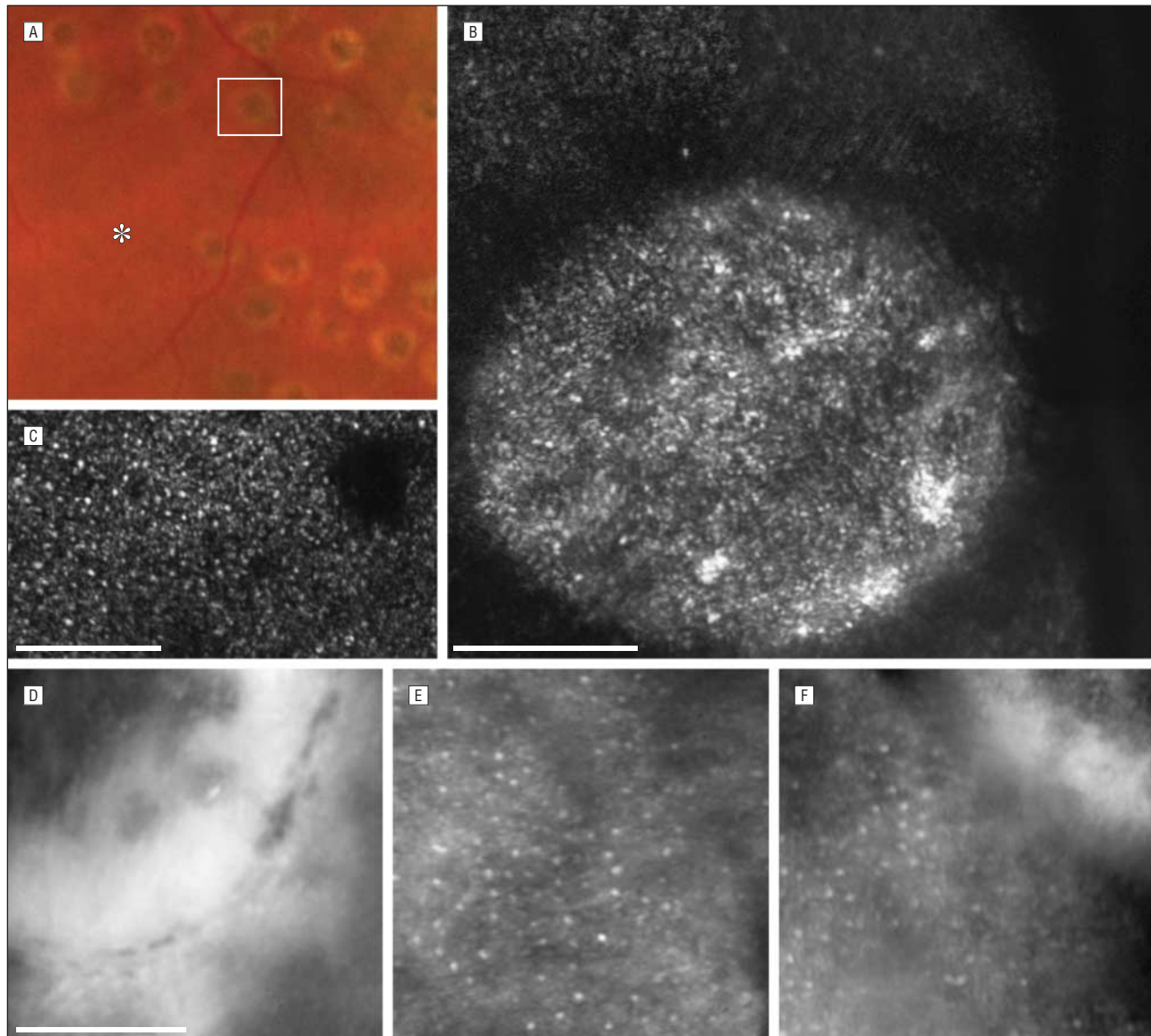


Figure 3. Images from subject 2. Color fundus photograph (A) with corresponding adaptive optics scanning ophthalmoscopic images of a 284- μm laser lesion obtained 216 days after panretinal laser photocoagulation (white box in A) (B) and a nearby normal-appearing location (asterisk in A) (C). Adaptive optics flood-illuminated images obtained 142 days after panretinal laser photocoagulation show diffuse hyperreflectivity at the edge of a lesion (D) and a normal-appearing mosaic in areas adjacent to lesions (E and F). Scale bars indicate 100 μm .

Comment. Using high-resolution retinal imaging, we evaluated the tissue response in the human eye to grid and focal laser treatment applied to achieve clinically accepted end points using the Pascal laser system. We detected no evidence of reduced photoreceptor density around the laser lesions, no apparent size reduction of the lesions relative to the initial application diameters, and thus no direct evidence of photoreceptor migration or healing. Reestablishment of the photoreceptor layer in areas of retinal photocoagulation has been observed in rabbit eyes subjected to Pascal laser lesions of barely visible to moderate intensity.¹⁰ We suspect that observed differences in photoreceptor healing relative to experimental studies may relate to differences among species, degree of pigmentation, cellular maturity, and variability in the grading of lesion intensities.

We are unaware of previously published reports of laser photocoagulation lesions in the living human eye evaluated using AO imaging. Furthermore, the discrimination between rods and cones, with each cell type having its own characteristic size and distribution elucidated by confocal AOSO,¹² is a unique aspect of this study that distinguishes it from other *in vivo* studies. The ability of AO imaging to directly assess photoreceptor structure with cellular resolution may facilitate new approaches to laser therapy, perhaps with the intent of preserving more photoreceptors.

Dennis P. Han, MD
 Jason A. Croskrey, BA
 Adam M. Dubis, BA
 Brett Schroeder, BS
 Jungtae Rha, PhD
 Joseph Carroll, PhD

Author Affiliations: Departments of Ophthalmology (Drs Han, Rha, and Carroll and Messrs Croskrey and Schroeder), Cell Biology, Neurobiology, and Anatomy (Mr Dubis and Dr Carroll), and Biophysics (Dr Carroll), Medical College of Wisconsin, Milwaukee.

Correspondence: Dr Han, Department of Ophthalmology, Medical College of Wisconsin, 925 N 87th St, Milwaukee, WI 53226 (dhan@mcw.edu).

Author Contributions: Dr Han had full access to all of the data in the study and takes responsibility for the integrity of the data and the accuracy of the data analysis.

Financial Disclosure: None reported.

Funding/Support: This work was supported by grants P30EY001931, T32EY014537, and R01EY017607 from the National Institutes of Health, an unrestricted departmental grant from Research to Prevent Blindness, the Thomas M. Aaberg Sr Retina Research Fund, and the Jack A. and Elaine D. Klieger Professorship in Ophthalmology (Dr Han). Mr Croskrey is the recipient of a Career Development Award from Research to Prevent Blindness. Temporary use of the Pascal laser was provided by OptiMedica Corp. This investigation was conducted in a facility constructed with support from grant C06 RR-RR016511 from the Research Facilities Improvement Program, National Center for Research Resources, National Institutes of Health.

Online-Only Material: The eFigures are available at <http://www.archophthalmol.com>.

Additional Contributions: Alfredo Dubra, PhD, designed the AOSO and Phyllis Summerfelt provided technical/administrative assistance in figure preparation.

1. Smiddy WE, Fine SL, Quigley HA, Hohman RM, Addicks EA. Comparison of krypton and argon laser photocoagulation: results of stimulated clinical treatment of primate retina. *Arch Ophthalmol*. 1984;102(7):1086-1092.
2. Smiddy WE, Fine SL, Green WR, Glaser BM. Clinicopathologic correlation of krypton red, argon blue-green, and argon green laser photocoagulation in the human fundus. *Retina*. 1984;4(1):15-21.
3. Marshall J, Bird AC. A comparative histopathological study of argon and krypton laser irradiations of the human retina. *Br J Ophthalmol*. 1979;63(10):657-668.
4. Toth CA, Birngruber R, Boppart SA, et al. Argon laser retinal lesions evaluated in vivo by optical coherence tomography. *Am J Ophthalmol*. 1997;123(2):188-198.
5. Framme C, Walter A, Prah P, et al. Structural changes of the retina after conventional laser photocoagulation and selective retina treatment (SRT) in spectral domain OCT. *Curr Eye Res*. 2009;34(7):568-579.
6. Kriechbaum K, Bolz M, Deak GG, Prager S, Scholda C, Schmidt-Erfurth U. High-resolution imaging of the human retina in vivo after scatter photocoagulation treatment using a semiautomated laser system. *Ophthalmology*. 2010;117(3):545-551.
7. Lanzetta P, Polito A, Veritti D. Subthreshold laser. *Ophthalmology*. 2008;115(1):216-216, e1.
8. Muqit MM, Gray JC, Marcellino GR, et al. Fundus autofluorescence and Fourier-domain optical coherence tomography imaging of 10 and 20 millisecond Pascal retinal photocoagulation treatment. *Br J Ophthalmol*. 2009;93(4):518-525.
9. Muqit MM, Gray JC, Marcellino GR, et al. In vivo laser-tissue interactions and healing responses from 20- vs 100-millisecond pulse Pascal photocoagulation burns. *Arch Ophthalmol*. 2010;128(4):448-455.
10. Paulus YM, Jain A, Gariano RF, et al. Healing of retinal photocoagulation lesions. *Invest Ophthalmol Vis Sci*. 2008;49(12):5540-5545.
11. Rha J, Schroeder B, Godara P, Carroll J. Variable optical activation of human cone photoreceptors visualized using a short coherence light source. *Opt Lett*. 2009;34(24):3782-3784.
12. Dubra A, Sulai Y, Norris JL, et al. Noninvasive imaging of the human rod photoreceptor mosaic using a confocal adaptive optics scanning ophthalmoscope. *Biomed Opt Express*. 2011;2(7):1864-1876.
13. Li KY, Roorda A. Automated identification of cone photoreceptors in adaptive optics retinal images. *J Opt Soc Am A Opt Image Sci Vis*. 2007;24(5):1358-1363.

Why Visual Function Does Not Correlate With Optic Glioma Size or Growth

It has long been known that little correlation exists between visual function and tumor size with respect to optic gliomas (World Health Organization grade I juvenile pilocytic astrocytomas).¹⁻³ Surprisingly, however, a deterioration in visual function in those harboring such masses is still often taken as clinical evidence of tumor progression and used to justify intervention for lesions that otherwise may have failed to demonstrate any growth.⁴

An understanding of why deterioration of clinical function may not be a sign of tumor progression but could actually indicate glioma regression may help to better resist physician and family impulses to intervene.⁵

Optic gliomas are congenital in origin. Masses formed within the central nervous system in utero may influence the subsequent apoptosis of excess axons,⁶ in effect molding themselves in relative harmony with remaining axons to allow maximal visual function despite the presence of what may otherwise appear to be an impressive tumor. Nonetheless, following the final organization of visual pathways, subsequent growth could alter such an in utero-established arrangement. Optic gliomas are also intrinsic to the optic nerve. Thus, the hamartomatous overgrowth of glial cells with supporting tissue elements that normally surround each axon, should it occur in uniform fashion, may not necessarily impede axoplasmic flow and neuronal signaling. Neurons remain functional and viable with elevated pressures uniformly distributed.^{7,8} Pressure applied focally, on the other hand, particularly from tumors arising extrinsic to a nerve, can easily create pressure gradients that pinch axons and block axoplasmic flow, thus producing subsequent atrophy.⁸ As an analogy, just as a human can withstand high pressure evenly distributed, such as is generated by several tons of water when near the bottom of a swimming pool, it could nonetheless poorly tolerate even a fraction of such pressure were it to be applied focally, such as by an elephant resting its foot on a person's torso (Alfredo A. Sadun, MD, PhD, oral communication, February 2009).

Hence, some optic gliomas can be large congenitally or noted to continue to grow to great extents along considerable lengths of the visual axonal pathways without causing any perceptible loss of visual acuity or function.¹⁻³ Others much smaller but with less uniform growth may compress or kink axons focally, causing considerable visual morbidity.¹⁻³

It should then be of no surprise that an intrinsic lesion shrinking in nonuniform fashion could also give rise to inhomogeneities and pressure gradients causing kinking of axons and loss of function,^{3,8} just as an enlarging tumor might do. Such an apparently paradoxical worsening of vision is acknowledged during the medical treatment of prolactinomas. While external compression of the chiasm may produce an